AGU FALL MEETING
San Francisco | 3–7 December 2012

Orientation effects in fault reactivation in geological CO_2 sequestration

Nicola Castelletto, Massimiliano Ferronato, Giuseppe Gambolati, Carlo Janna, Pietro Teatini
Department of Civil, Environmental and Architectural Engineering, University of Padova - Via Trieste 63, 35121 Padova (PD), Italy
{nicola.castelletto, massimiliano.ferronato, giuseppe.gambolati, carlo.janna, pietro.teatini}@unipd.it

Poster H23D-1388

Università degli Studi di Padova

Abstract

Geological CO_2 sequestration remains one of the most promising option for reducing the greenhouse gases emission. The accurate simulation of the complex coupled physical processes occurring during the injection and the post-injection stage represents a key issue for investigating the feasibility and the safety of the sequestration. Recently, the importance of geomechanical processes has been widely recognized. In the present modeling study, we focus on fault reactivation induced by injection, an essential aspect for the evaluation of CO_2 sequestration projects that needs to be adequately investigated to avoid the generation of preferential leaking path for CO_2 and the related risk of induced seismicity. We use a geomechanical model based on the structural equations of poromechanics solved by the Finite Element (FE) - Interface Finite Element (IFE) approach. Standard FEs are used to represent a continuum, while IFEs prove especially suited to assess the relative displacements of adjacent elements such as the opening and slippage of existing faults or the generation of new fractures. The model is used to address the reactivation of a single fault in a synthetic reservoir and successfully experimented with in a real application.

1. Geomechanical model governing equations

Assuming small deformation and isothermal conditions, the quasi-static equations governing the mechanical equilibrium on a three-dimensional spatial domain Ω can be written as:

$$\nabla \cdot \boldsymbol{\sigma} + \rho_b \mathbf{g} = \mathbf{0} \tag{1}$$

with $\mathbf{g}$ gravity, $\rho_b = \left[\phi\rho_f + (1-\phi)\rho_s\right]$ the bulk density, ρ_f the total fluid density, ρ_s the solid-phase density, ϕ porosity, and $\nabla\cdot$ the divergence operator. The total-stress $\boldsymbol{\sigma}$ is given by the following relationship [e.g., 1]:

$$\boldsymbol{\sigma} - \boldsymbol{\sigma}_0 = \mathbf{C} : \boldsymbol{\varepsilon} - b\left(p_f - p_{f,0}\right)\mathbf{1} \tag{2}$$

where $\mathbf{C}$ is the fourth-order stiffness tensor of the solid matrix, $\boldsymbol{\varepsilon} = \left[\left(\nabla\hat{\mathbf{u}} + \nabla^T\hat{\mathbf{u}}\right)/2\right]$ is the second-order strain tensor, with $\hat{\mathbf{u}}$ the displacement vector and ∇ the gradient operator, b is the Biot coefficient, **1** is the second-order identity tensor, and the subscript 0 denotes the reference state. The fluid pressure p_f has to take into account the pressure of both the wetting (p_w) and the non-wetting (p_g) phase according to the following definition [2]:

$$p_f = p_g - S_w\left(p_g - p_w\right) = S_g p_g + S_w p_w \tag{3}$$

with S_w and S_g the saturation index of water and gas, respectively. In the present analysis, the porous medium is considered isotropic. The constitutive relationship (2) may be rewritten in the following form [3]:

$$\begin{aligned}\boldsymbol{\sigma} - \boldsymbol{\sigma}_0 = {} & \frac{E}{(1+\nu)(1-2\nu)}\left[(1-2\nu)\boldsymbol{\varepsilon} + \nu\,\mathrm{trace}(\boldsymbol{\varepsilon})\,\mathbf{1}\right] - \\ & b\left[\left(S_g p_g + S_w p_w\right) - \left(S_{g_0} p_{g_0} + S_{w_0} p_{w_0}\right)\right]\mathbf{1}\end{aligned} \tag{4}$$

where the tensor $\mathbf{C}$ is expressed as a function of the Poisson ratio ν and the Young modulus E.

2. Numerical model: Finite Elements and Interface Elements

The geomechanical response of a formation subject to CO_2 injection is investigated by a one-way coupling approach. The differential system (1) is solved numerically by finite elements (FEs) using the GEPS3D (Geomechanical Elasto-Plastic 3D Simulator) code, developed at the University of Padova, following the infinite pore pressure gradient formulation [4].
Fault/thrust mechanics is simulated in GEPS3D with the aid of special IFEs recently developed in [5] for the simulation of contact surfaces in porous media, and already used in a number of realistic applications [e.g., 3]. The IFEs implemented herein are six-node isoparametric zero-thickness elements, compatible with linear and bilinear FEs, and consist of a pair of linear elements in which the opposite nodes coincide. Top and bottom of the element represent the contact surfaces with nodes i, j and k initially coinciding with nodes l, m and n (Fig. 1).

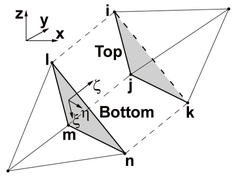

Figure 1: *Sketch of a six-node isoparametric interface element within a 3D FE grid with the local reference frame (ξ-η-ζ) associated with each element highlighted.*

An elastoplastic constitutive law is adopted assuming a Mohr-Coulomb failure criterion as the yield surface F:

$$F = \tau_s - \tau_s^F \qquad \text{with:} \begin{cases} \sigma_n \le 0 \\ \tau_s = \sqrt{\tau_{s1}^2 + \tau_{s2}^2} \\ \tau_s^F = -\sigma_n \tan\phi_f + c_f \end{cases} \tag{5}$$

where the plastic-flow-rule potential G is such that $\partial G/\partial\sigma_n = 0$ and $\partial G/\partial\tau_s = \pm 1$, with σ_n the normal stress (negative in compression, positive in expansion) and τ_{s1} and τ_{s2} the shear stress components in the interface plane the normal, ϕ_f and c_f the fault friction angle and cohesion, respectively.
Assuming the nodal displacement $\mathbf{u}$ as primary unknowns, the final nonlinear system to be solved can be generally written as:

$$\left[\mathbf{K}_m + \mathbf{K}_i\right]\mathbf{u} = \mathbf{f}(t) \tag{6}$$

where $\mathbf{K}_m$ is the global stiffness matrix obtained from assembling the contribution from the traditional linear or bilinear finite elements, $\mathbf{K}_i$ is the global stiffness matrix generated from the interface elements, and $\mathbf{f}(t)$ is the global forces vector depending on time t. Matrices $\mathbf{K}_m$ and $\mathbf{K}_i$ generally depend on the stress tensor, hence the solution vector $\mathbf{u}$, giving rise to a highly nonlinear problem. For a detailed description of the solution algorithm, see [5].

3. Numerical results

Fluid is injected in a deep formation from an infinite number of aligned injection wells. A normal fault with orientation α intersects the storage formation at about 500 m from the injection point (Fig. 2).

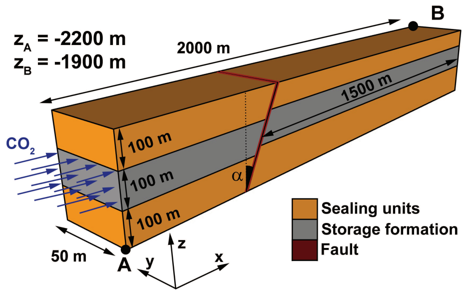

Figure 2: *Sketch of the integration domain.*

An unstructured mesh totalling approximatively 12,100 nodes, 54,300 FEs and 200 IFEs is used. The following assumptions hold:

- the storage formation is confined on top and bottom by impermeable units and faults are considered not hydraulically conductive;
- roller constraints are prescribed on the lateral boundary with a traction-free plane on top and a zero displacement bottom;
- the overburden density gradient is equal to 10^{-2} MPa/m, with the maximum σ_1 and minimum σ_3 principal stresses set equal to the vertical σ_v and horizontal σ_h stresses, respectively;
- the geo-mechanical properties are uniform in both the sealing and the storage units, with E = 2.0 GPa, ν = 0.3, b = 1.0, while c_f is varied between 0.0 and 1.0 MPa, and ϕ_f from 25° to 35°;
- a constant pore pressure buildup equal to 8.0 MPa is prescribed within the injected unit, namely 40% beyond the initial hydrostatic value.

The numerical simulations aim at exploring the influence of fault orientation α and the initial ratio $\sigma_{h,0}/\sigma_{v,0}$ on fault slippage activation. The results are summarized in Figs. 3-5.

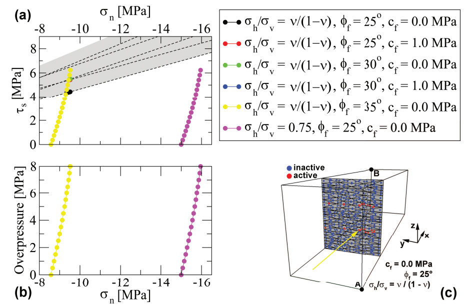

Figure 3: *Fault slip activation at Gauss points (c) for c_f=0.0 MPa, ϕ_f=25° (i.e. the least conservative case) and $\sigma_h/\sigma_v = \nu/(1-\nu)$ = 0.43 for the vertical fault case (α=0°). Stress path (a) in the (σ_n-τ_s)-space, for the Gauss point highlighted by the yellow arrow in (c), for other choices of the pair (c_f-ϕ_f) and the ratio σ_h/σ_v. The behavior of the normal stress σ_n vs. overpressure is also plotted.*

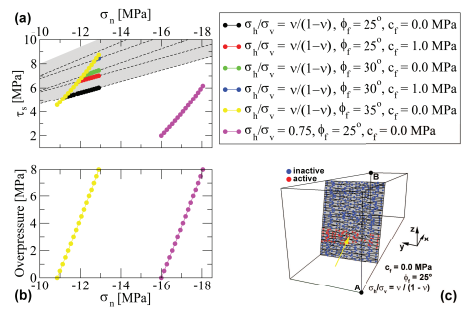

Figure 4: *The same as Fig. 3 for α=30°.*

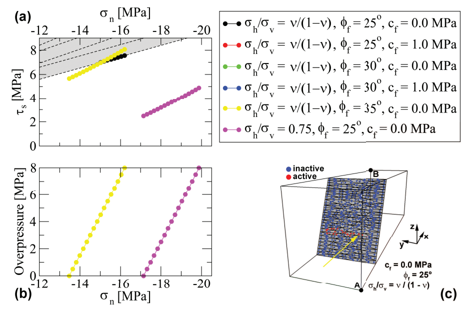

Figure 5: *The same as Fig. 3 for α=60°.*

4. Real field application

The present real field example shows some results concerning fault activation in a geomechanical simulation carried out to investigate the safety of the CO_2 sequestration in a deep saline aquifer at a depth ranging between 2500 and 3000 m (Fig. 6).

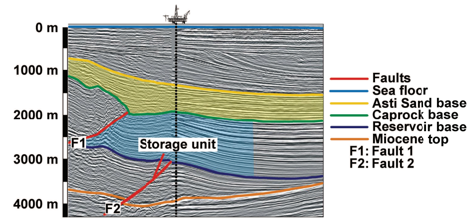

Figure 6: *Seismic section of the storage structure showing the depth of the major horizons and faults.*

The storage reservoir is tested as a possible site of CO_2 disposal for one of the six CO_2 CCS demonstration projects that have been selected by the European Energy Programme for Recovery (EEPR). It is a large scale project aimed at implementing the CCS technology at one of the three 660×10^6 W units of an existing power plant in Italy. An injection rate of 1×10^6 ton/a of CO_2 over 10 years is required [6, 7].
The faulted geological structure is accurately reproduced based on detailed seismic surveys (Figs. 7-9).

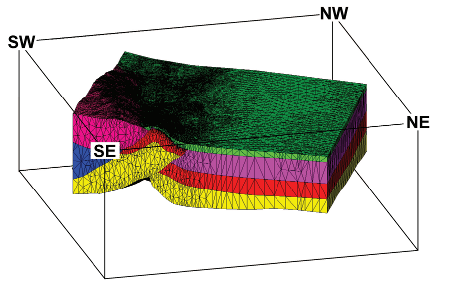

Figure 7: *3D FE-IE mesh of the storage structure. The colors are representative of the different geologic units. Vertical exaggeration is 2.*

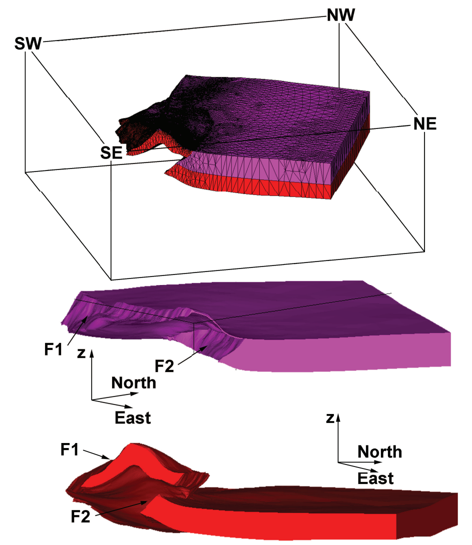

Figure 8: *Detail of the portion 3D FE-IE showing the two units where CO_2 injection is planned. The dislocation along discontinuities F1 and F2 is highlighted. Vertical exaggeration is 2.*

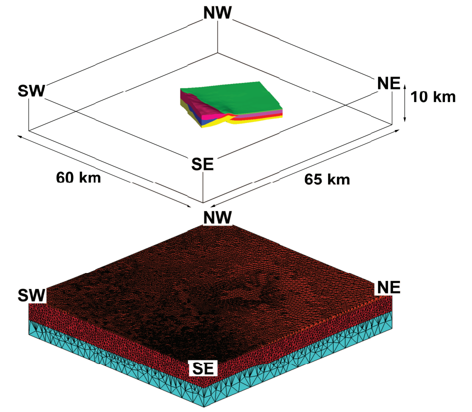

Figure 9: *Sketch representing the storage structure within the (black) box representing the domain selected for the geomechanical modelling (top). Perspective view of the 3D grid of simulated domain, totalling 376,640 nodes, 2,196,495 FEs and 37,608 IFEs.*

The pore pressure distribution due to a single injection well is provided by a fluid-dynamic simulator. Fig. 10 shows the predicted overpressure at the well location at several time steps.

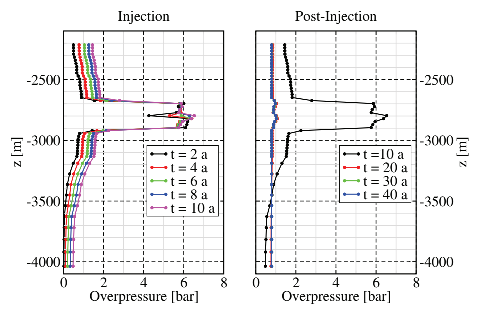

Figure 10: *Expected overpressure distribution at the injection well during the injection (left) and the post-injection (right) stage, respectively.*

The following assumptions hold:

- a hypoplastic constitutive law derived from radioactive marker measurements carried out in the Adriatic Sea [8] is selected for the geomechanical characterization of the porous formation;
- the horizontal stresses σ_h are assumed to be isotropic and derived from the vertical stress $\sigma_v = \sigma_z$ using the confinement factor $\kappa = \nu/(1-\nu)$;
- concerning the failure criterion, as no direct measurements are available to characterize the yield surface relative to the faults, no cohesion (c_f = 0.0 bar) and a friction angle ϕ_f = 30° are assumed.

The prediction has been extended up to 20 years after the inception of pumping. The initial stress state acting on the faults surfaces is given in Fig. 11a,e. The results provided by GEPS3D after 2, 10 and 20 years from the inception of injection are shown in Fig. 11. The figure shows the values of the stress normal and tangential to the faults, respectively. Both faults activate neither to tensile opening nor to shear sliding.

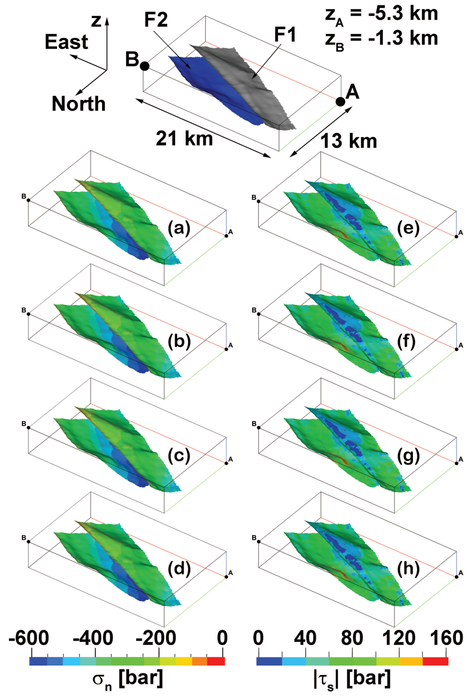

Figure 11: *Faults in the storage structure (top). Initial value of the stress σ_n normal to the fault surfaces (a) and value of the stress τ_s tangential to the faults surfaces (e) assuming a normally consolidated basin. Values of σ_n and τ_s after 2 (b,f), 10 (c,g) and 20 (d,h) years from the injection inception.*

References

[1] Coussy O. *Poromechanics*. Wiley: Chichester, 2004.

[2] Bishop AW. The principle of effective stress. *Teknisk Ukebla* 1959; **39**:859–863.

[3] Ferronato M, Gambolati G, Janna C, Teatini P. Geomechanical issues of anthropogenic CO_2 sequestration in exploited gas fields. *Energy Conv. Manag.* 2010; **51**(10):1918–1928.

[4] Gambolati G, Ferronato M, Teatini P, Deidda R, Lecca G. Finite element analysis of land subsidence above depleted reservoirs with pore pressure gradient and total stress formulations. *Int. J. Numer. Anal. Methods Geomech.* 2001; **25**(4):307–327.

[5] Ferronato M, Gambolati G, Janna C, Teatini P. Numerical modeling of regional faults in land subsidence prediction above gas/oil reservoirs. *Int. J. Numer. Anal. Methods Geomech.* 2008; **32**:633–657.

[6] Castelletto N, Gambolati G, Teatini P. Geological CO_2 sequestration in multi-compartment reservoirs: geomechanical challenges. Submitted for publication.

[7] Castelletto N, Teatini P, Gambolati G, Bossie-Codreanu D, Olivier V, et al. Multiphysics modeling of CO_2 sequestration in a faulted saline formation in Italy. Submitted for publication.

[8] Baù D, Ferronato M, Gambolati G, Teatini P. Basin-scale compressibility of the northern Adriatic by the radioactive marker technique. *Geotechnique* 2002; **52**(8):605–616.